

---

# LARGE LANGUAGE MODEL GUIDED INCENTIVE AWARE REWARD DESIGN FOR COOPERATIVE MULTI-AGENT REINFORCEMENT LEARNING \*

---

**Doğan Urgan**

Department of Electrical and Electronics Engineering  
Karabuk University  
78050 Karabuk, Türkiye  
durgun@karabuk.edu.tr

**Gokhan Gungor**

Department of Mechatronics Engineering  
Karabuk University  
78050 Karabuk, Türkiye  
gokhangungor@karabuk.edu.tr

## ABSTRACT

Designing effective auxiliary rewards for cooperative multi-agent systems remains a precarious task; misaligned incentives risk inducing suboptimal coordination, especially where sparse task feedback fails to provide sufficient grounding. This study introduces an automated reward design framework that leverages large language models to synthesize executable reward programs from environment instrumentation. The procedure constrains candidate programs within a formal validity envelope and evaluates their efficacy by training policies from scratch under a fixed computational budget; selection depends exclusively on the sparse task return. The framework is evaluated across four distinct Overcooked-AI layouts characterized by varied corridor congestion, handoff dependencies, and structural asymmetries. Iterative search generations consistently yield superior task returns and delivery counts, with the most pronounced gains occurring in environments dominated by interaction bottlenecks. Diagnostic analysis of the synthesized shaping components indicates increased interdependence in action selection and improved signal alignment in coordination-intensive tasks. These results demonstrate that the search for objective-grounded reward programs can mitigate the burden of manual engineering while producing shaping signals compatible with cooperative learning under finite budgets.

**Keywords** Deep learning · large language models · multi-agent learning · reinforcement learning · reward shaping

## 1 Introduction

Reward specification remains a primary bottleneck in reinforcement learning (RL). In many domains, the intended objective is inherently sparse or delayed; consequently, empirical performance often depends more on the design of auxiliary feedback than on improvements to the optimization algorithm itself. In cooperative multi-agent reinforcement learning (MARL), this challenge is further amplified: as agents interact within a Markov game [1], auxiliary rewards influence not only credit assignment and exploration, but also the incentives necessary for coordination. As a result, reward shaping that accelerates learning in one setting can induce brittle strategies in another, including behaviors that maximize a proxy signal while failing to improve the true task return.

A formal framework for reward shaping is provided by potential-based reward transformations, which augment the reward with a shaped term defined as the discounted difference of a potential function across transitions. Such transformations are known to preserve the set of optimal policies under standard assumptions, such as the use of a consistent discount factor and a state-dependent potential function [2]. This policy-invariance property clarifies the conditions under which an auxiliary learning signal can be introduced without altering the true objective. Although subsequent research expanded the framework to incorporate richer features, such as state-action formulations [3], and extended it to multi-agent settings [4], such formal advances do not alleviate the practical burden of specifying an

---

\*This work is currently under peer review.

effective potential function. Furthermore, they fail to cover the broad class of heuristic event bonuses and penalties commonly used in applied systems.

Beyond theoretical limitations, the reliance of deep RL on function approximation and finite training budgets renders optimization dynamics highly sensitive to auxiliary rewards; accordingly, theoretically policy-invariant shaping may still yield mixed empirical outcomes in complex multi-agent settings [5]. Consequently, reward shaping typically requires extensive manual tuning, and the potential for reward misspecification remains a recurring concern. At the core of this challenge lies a fundamental mismatch between the implemented reward and the intended objective, which is formally addressed by inverse reward design. By treating the specified reward as evidence of intent that requires contextual interpretation, this approach reveals that optimizing an underspecified proxy can lead to unintended side effects [6], thereby necessitating that automated reward design methods be used against the true objective, rather than the auxiliary signals they generate.

To mitigate the reliance on manual engineering, data-driven paradigms attempt to automate reward design by learning functional representations directly from demonstrations or feedback. Inverse Reinforcement Learning (IRL) operationalizes this by inferring underlying reward functions from expert trajectories [7-8], while preference-based learning recovers reward signals through pairwise comparisons of trajectory segments [9]. Although these approaches are powerful when high-quality demonstrations or labels are accessible, they entail substantial data collection and interface overhead, which often proves prohibitive in complex, simulation-heavy MARL environments. Furthermore, even when a shaping reward is provided, its efficacy often varies across the state space. This inconsistency requires methods that determine when and how much to rely on shaping [10].

Large Language Models (LLMs) emerge as a scalable alternative to data-intensive methods, offering a path toward automated reward generation without the overhead of human-in-the-loop labeling. Transformers facilitate robust conditional generation [11], and large-scale pretrained models demonstrate broad competence in program synthesis from structured context [12]. Recent advances in code generation further support the feasibility of producing nontrivial executable artifacts from natural language specifications [13]. Based on these capabilities, recent frameworks utilize LLMs to propose reward programs that improve through empirical feedback in RL settings [14]. LLMs also facilitate the production of shaped reward programs from language-conditioned task descriptions [15]. Nevertheless, autonomous reward generation presents two primary technical challenges: generated functions require basic correctness and boundedness, while candidate rewards require objective-aligned evaluation to mitigate the risk of optimizing spurious proxies.

To address these requirements, this work introduces an LLM-guided reward shaping search framework for cooperative MARL. The proposed approach represents reward function candidates as executable programs, evaluates them through end-to-end training against a fixed baseline, and selects the optimal candidates based solely on the sparse task objective. By doing so, the framework ensures that the shaping signals remain grounded in the true mission goal while leveraging the generative prior of LLMs. We evaluate this method on a standard cooperative coordination benchmark across multiple tasks and analyze the resulting reward candidates to characterize their impact on multi-agent coordination.

The contributions of this work are threefold. First, we introduce an automated reward search framework for cooperative MARL that leverages objective-grounded selection to ensure alignment with global goals. Second, we provide empirical validation across four coordination tasks, incorporating incentive diagnostics to characterize the signals induced by candidate rewards. Finally, we present a systematic diagnostic analysis that illustrates how synthesized reward functions shape specific coordination behaviors and influence the underlying multi-agent learning dynamics.

## 2 Related Work

Reduction of reward engineering has been studied from several perspectives, including reward shaping and credit assignment in cooperative MARL, reward construction or optimization from data and interaction, and programmatic reward generation using LLMs. Reward shaping remains a common practical tool for accelerating learning with sparse objectives, but it introduces design choices that can change learning dynamics and, in multi-agent settings, can change incentives. Policy-invariant shaping provides a principled baseline for adding auxiliary signal without altering the underlying objective [2], and later work broadens the class of potential-based constructions [3]. In cooperative MARL, the reward signal also serves as a mechanism for credit assignment, motivating designs that better reflect each agent’s contribution to team performance; potential-based difference rewards are an example of this direction [4]. These lines of work clarify that auxiliary rewards can be useful, but they do not remove the need to specify effective shaping terms for a given domain, nor do they ensure that heuristically chosen event-based shaping will avoid proxy optimization.

A second set of methods aims to reduce manual tuning by modifying or learning how rewards are used during training. Some approaches explicitly optimize the reward function so that, under a fixed learning procedure, the induced behavior

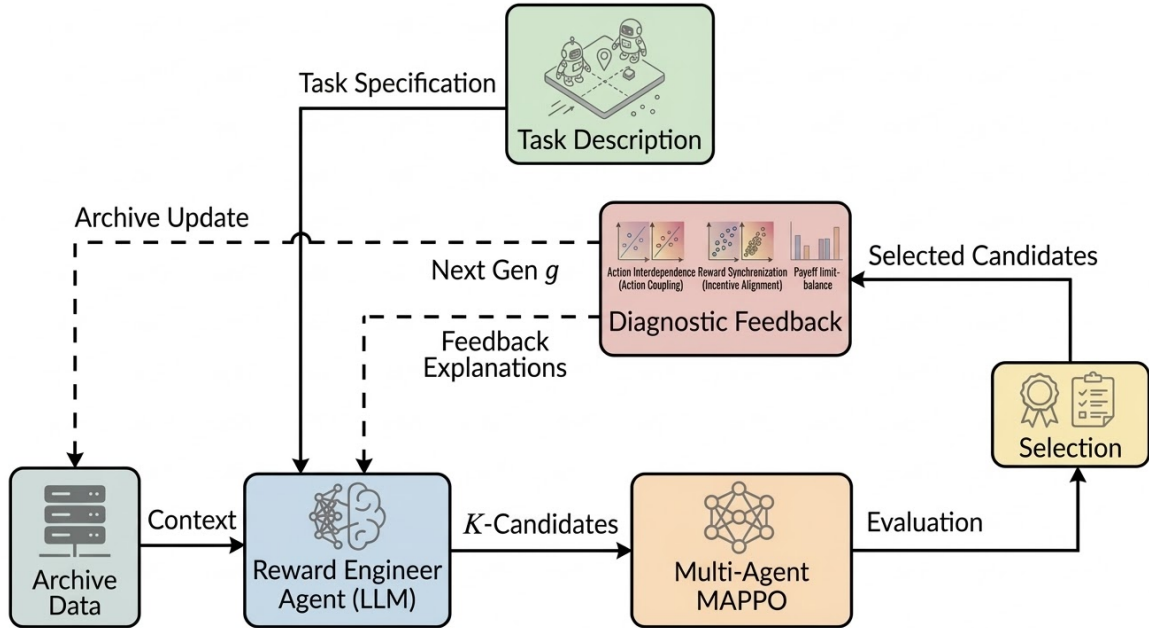


Figure 1: The proposed objective-grounded reward search framework.

better matches a target notion of alignment [16]. Other work studies how an agent can learn to rely on shaping rewards selectively when shaping quality varies across the state space [10]. These approaches motivate two design choices adopted in the present work: reward candidates are evaluated through end-to-end training under a fixed baseline, and selection is performed using the true task objective rather than the shaped signal. Reward specification can also be addressed by inferring objectives from demonstrations or feedback. Inverse RL infers a reward function from expert behavior [7-8], and preference-based learning infers rewards from human comparisons [9]. Such methods reduce the need to handcraft shaping terms, but require demonstrations, preferences, or interactive supervision. The present work targets a complementary regime in which repeated simulation and environment instrumentation are available and in which reward candidates can be tested by training and evaluation without collecting additional human labels.

Recent work has leveraged LLMs to generate executable artifacts, enabled by Transformer-based conditional generation [11-12], and demonstrated in general-purpose code synthesis [13]. Building on these capabilities, LLMs have been used to propose reward programs that are improved through empirical feedback in RL [14], and to generate shaped reward programs from task descriptions [15]. Our approach diverges from these frameworks in two aspects critical to cooperative MARL: candidate rewards are executable programs over instrumentation signals, and candidates are accepted only when they improve the sparse task objective under a fixed multi-agent learning baseline, which is intended to limit proxy optimization effects [6].

### 3 Method

The general framework of the proposed method is illustrated in fig. 1. The system implements an iterative, closed-loop reward engineering process that leverages the generative capabilities of LLMs and the evaluative precision of MARL. An objective-grounded reward search procedure is described for cooperative MARL. At a high level, an LLM proposes executable reward candidates conditioned on a structured task description and an archive of prior outcomes. Each candidate is constrained by a validity envelope that enforces implementability and discourages exploitable proxies. Valid candidates are used to train policies from scratch with a fixed MARL learner under a fixed budget, and their performance is evaluated solely with the sparse task objective. In addition, descriptive incentive diagnostics are computed from rollouts and used as structured feedback for subsequent candidate generation.

### 3.1 Problem Setting and Reward Interfaces

We consider a cooperative Markov game [1] defined by the tuple  $\mathcal{G} = \langle \mathcal{S}, \{\mathcal{A}_i\}_{i=1}^n, \mathbf{P}, r_{\text{sparse}}, \gamma \rangle$ , with  $n$  agents interacting in the state space  $\mathcal{S}$ . At each time step  $t$ , the environment is in state  $s_t \in \mathcal{S}$ . Each agent  $i \in \{1, \dots, n\}$  selects an action  $a_{t,i}$  from its individual action space  $\mathcal{A}_i$ , forming a joint action  $\mathbf{a}_t = (a_{t,1}, \dots, a_{t,n}) \in \mathcal{A}$ , where  $\mathcal{A}$  is the joint action space. The system dynamics follow the transition probability kernel  $\mathbf{P} : \mathcal{S} \times \mathcal{A} \times \mathcal{S} \rightarrow [0, 1]$ , which defines the probability  $\mathbf{P}(s_{t+1} | s_t, \mathbf{a}_t)$  of transitioning to state  $s_{t+1}$  given the current state  $s_t$  and joint action  $\mathbf{a}_t$ . Furthermore,  $r_{\text{sparse}} : \mathcal{S} \times \mathcal{A} \rightarrow \mathbb{R}$  defines the reward function for shared sparse tasks, and  $\gamma \in [0, 1]$  is the discount factor.

In this cooperative setting, the task reward is sparse and shared; specifically, a scalar reward  $r_{\text{sparse},t} = r_{\text{sparse}}(s_t, \mathbf{a}_t)$  is produced by the environment and assigned equally to all agents. The performance objective is to maximize the expected discounted sparse return:

$$J(\pi) = \mathbb{E}_{\tau \sim \pi} \left[ \sum_{t=0}^{T-1} \gamma^t r_{\text{sparse},t} \right], \quad (1)$$

where  $\pi$  denotes the joint policy,  $\tau$  represents a trajectory induced by  $\pi$ , and  $T$  is the episode horizon.

In addition to the sparse reward, the simulator exposes structured instrumentation through an information record  $\text{info}_t$ . A deterministic feature map  $\phi$  is used to convert the transition and instrumentation into a feature vector,

$$\mathbf{x}_t = \phi(s_t, \mathbf{a}_t, s_{t+1}, \text{info}_t). \quad (2)$$

A reward candidate is represented as an executable program  $p$  that produces agent-specific shaping signals from the instrumentation. Given the state features  $\mathbf{x}_t$  and the global sparse task reward  $r_{\text{sparse},t}$ , the program generates a vector of auxiliary shaping

$$\mathbf{r}_t^{(p)} = p(\mathbf{x}_t, r_{\text{sparse},t}) \in \mathbb{R}^n, \quad (3)$$

where the  $i$ -th component  $r_{t,i}^{(p)}$  denotes the shaping signal assigned to agent  $i$  at step  $t$ . During training, each agent receives an augmented reward

$$\tilde{r}_{t,i} = r_{\text{sparse},t} + \lambda r_{t,i}^{(p)}, \quad (4)$$

where  $\lambda \geq 0$  is the fixed scaling factor. The sparse reward term preserves the intended task objective, while the shaping term is used only to improve learning under finite budgets. In all results reported, the candidates are compared using the sparse objective in eq. (1), not the shaped return.

### 3.2 Objective-Grounded Search and Selection

Let  $\text{Train}(\cdot; \boldsymbol{\theta}, \xi)$  denote training with a fixed MARL learner (MAPPO) using fixed hyperparameters  $\boldsymbol{\theta}$  and randomness  $\xi$ . The candidate evaluation process adheres to the Centralized Training, Decentralized Execution (CTDE) paradigm, as illustrated in fig. 2. During the centralized training phase (fig. 2a), a centralized critic  $\mathbf{V}$  leverages a shared buffer of global states and joint observations to evaluate the collective policy and derive training feedback. This centralized value estimate is utilized to provide advantage signals that guide the policy updates for all agents. Conversely, during the decentralized execution phase (fig. 2b), the decentralized actors  $\pi_i$  select actions based strictly on local observations. Upon completion of training with the augmented rewards defined in eq. (4), the candidate is evaluated exclusively via the sparse task objective  $\mathcal{G}$  to obtain the empirical estimate  $\widehat{J}(p)$ .

The search process evolves over a total of  $G$  generations. At each generation index  $g \in \{1, \dots, G\}$ , a structured context  $c_g$  is constructed from the task description, the instrumentation schema, the reward interface, and summaries of previously evaluated candidates. The LLM proposes  $K$  reward candidates by sampling from a conditional distribution  $q_\psi(p | c_g)$ . Each candidate  $p$  is filtered by a validity envelope before training. The envelope enforces correct input and output signatures, determinism, bounded outputs via clipping, and robustness to missing instrumentation keys. Candidates failing validation are rejected, and when failures are syntactic or runtime in nature, a bounded number of repair attempts are performed by conditioning on the error trace.

Within each generation, candidates are trained and evaluated, and the best candidate is selected based on the sparse return:

$$p_g^* \in \arg \max_{k \in \mathcal{V}_g} \widehat{J}(p_{g,k}), \quad (5)$$

where  $p_{g,k}$  is the  $k$ -th candidate in generation  $g$  for  $k \in \mathcal{V}_g \subseteq \{1, \dots, K\}$ , and  $\mathcal{V}_g$  denotes the set of indices for candidates that pass validation. Selection is objective-grounded because only the sparse return is used for promotion. The complete procedure, which encompasses LLM-based iterative reward generation and the inner MARL evaluation loop, is summarized in Algorithm 1.

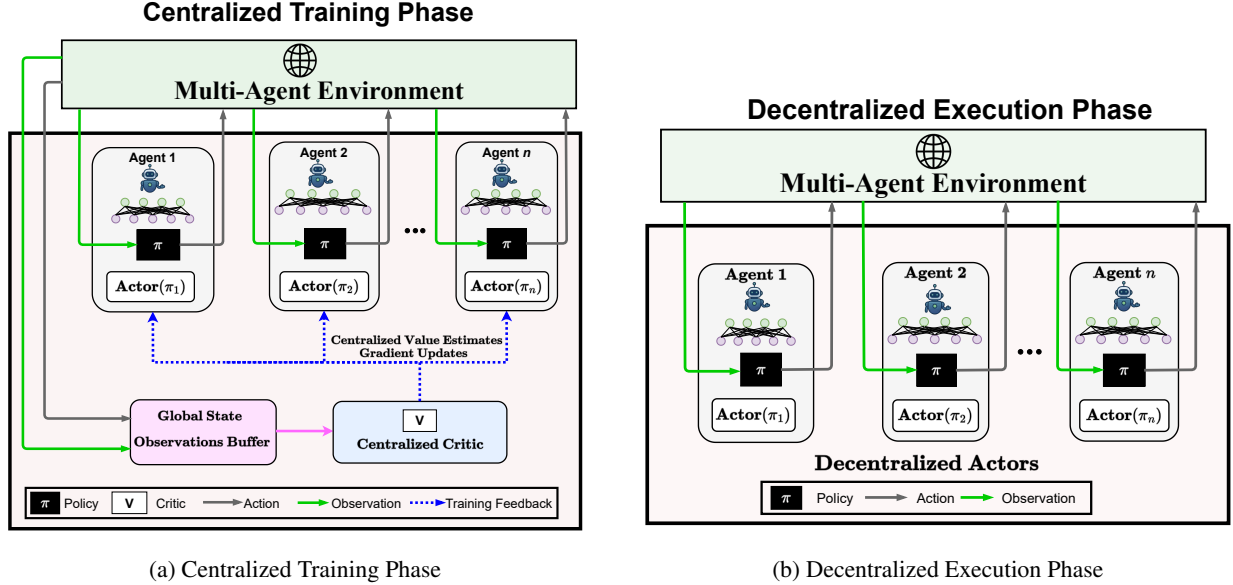


Figure 2: Overview of the CTDE paradigm for multi-agent reinforcement learning. (a) Centralized Training: A shared critic ( $V$ ) utilizes global state information and joint observation buffers to guide policy updates via training feedback. (b) Decentralized Execution: Individual actors ( $\pi_i$ ) rely exclusively on local observations for action selection, ensuring scalability in partially observable environments.

---

**Algorithm 1:** Objective-grounded incentive-aware reward search.

---

**Require :** Task specification and instrumentation schema; validity envelope; learner settings  $\theta$ ; generations  $G$ ; candidates per generation  $K$

```

1 Initialize archive  $\mathcal{A} \leftarrow \emptyset$ , and best score  $\hat{J}_{\text{best}} \leftarrow -\infty$ 
2 for  $g = 1$  to  $G$  do
3   Construct context  $c_g$  from task description and archive summaries
4   Sample candidates  $\{p_{g,k}\}_{k=1}^K \sim q_\psi(p | c_g)$ 
5   for  $k = 1$  to  $K$  do
6     Validate and, if needed, repair  $p_{g,k}$ 
7     if  $p_{g,k}$  is valid then
8       Train policy  $\pi_{g,k} \leftarrow \text{Train}(\cdot; \theta, \xi)$  using augmented rewards  $\tilde{r}_{t,i}$ 
9       Evaluate estimate  $\hat{J}(p_{g,k})$  using sparse reward only
10      Compute diagnostics  $d(p_{g,k})$  from rollouts
11       $\mathcal{A} \leftarrow \mathcal{A} \cup \{(p_{g,k}, \hat{J}(p_{g,k}), d(p_{g,k}))\}$ 
12    end if
13  end for
14  Update context summaries in  $\mathcal{A}$ 
15 end for

```

**Return :** Best candidate  $p^* = \arg \max_{(p, \cdot) \in \mathcal{A}} \hat{J}(p)$

---

### 3.3 Incentive Diagnostics Used for Feedback

The candidate program can assign different shaping signals to different agents, even when the task objective is shared. For interpretability, the shaping component is analyzed separately from the sparse reward. Using the agent-specific shaping signal  $r_{t,i}^{(p)}$ , the discounted shaping return for agent  $i$  on a rollout is defined as:

$$S_i(p) = \sum_{t=0}^{T-1} \gamma^t r_{t,i}^{(p)}. \quad (6)$$

These returns are computed on the shaping component only and therefore can be asymmetric even when the environment reward is a shared team reward.

### 3.3.1 Payoff imbalance.

Payoff imbalance measures the disparity in shaping returns across  $n$  agents. To ensure the metric remains bounded and interpretable, we define it as the normalized sum of all-pairs differences:

$$\Delta(p) = \frac{\sum_{i=1}^n \sum_{j=i+1}^n |S_i(p) - S_j(p)|}{(n-1) \sum_{k=1}^n |S_k(p)| + \varepsilon}, \quad (7)$$

where  $\varepsilon > 0$  is a small constant for numerical stability. This formulation is bounded within  $[0, 1]$ , where  $\Delta(p) \rightarrow 0$  indicates a symmetric distribution of rewards and larger values signal a disproportionate concentration on a subset of agents.

### 3.3.2 Incentive alignment

Incentive alignment measures the degree to which per-step shaping signals concurrently reinforce the agents. For an ensemble of  $n$  agents, we define this as the average pairwise Pearson correlation across all time steps in an episode:

$$\rho(p) = \frac{2}{n(n-1)} \sum_{i=1}^n \sum_{j=i+1}^n \text{corr}(r_{t,i}^{(p)}, r_{t,j}^{(p)}). \quad (8)$$

Strongly positive values ( $\rho \rightarrow 1$ ) indicate that the shaping signals are synchronized, suggesting that the reward program  $p$  induces mutually reinforcing behaviors. Conversely, values near zero or negative suggest decoupled or conflicting incentives, potentially signaling a breakdown in cooperative dynamics or the optimization of competitive proxy goals.

### 3.3.3 Action Coupling

Action coupling quantifies the statistical dependence between the agents’ decision-making processes under the policy optimized via program  $p$ . For an ensemble of  $n$  agents, we report the average pairwise Normalized Mutual Information (NMI) across all time steps:

$$\text{NMI}(p) = \frac{2}{n(n-1)} \sum_{i=1}^n \sum_{j=i+1}^n \frac{I(A_i; A_j)}{\sqrt{H(A_i)H(A_j)}}, \quad (9)$$

where  $I(A_i; A_j)$  denotes the mutual information between the action distributions of agents  $i$  and  $j$ , and  $H(A_i)$  represents the marginal entropy of the discrete action random variable  $A_i$  estimated from rollout data. Unlike raw mutual information, this geometric mean normalization ensures the metric is bounded within  $[0, 1]$ , where higher NMI indicates more interdependent action selection. This serves as a proxy for identifying whether the synthesized reward signals induce emergent coordination or lead to independent, decoupled strategies.

### 3.3.4 Diagnostic Feedback and Logging

Upon the completion of each evaluation rollout, the framework logs a comprehensive diagnostic tuple for every candidate:

$$d(p) = (\hat{J}(p), \Delta(p), \rho(p), \text{NMI}(p)), \quad (10)$$

which characterizes the candidate’s performance, payoff distribution, signal alignment, and behavioral coupling, respectively. While these diagnostics serve as high-dimensional descriptive feedback to guide the LLM proposer in subsequent generations, the final selection and promotion mechanism remains strictly exclusive to the sparse task return  $\hat{J}(p)$ . This decoupling ensures that while the search process is informed by complex coordination metrics, the optimization objective remains grounded in the true environment goal, preventing the emergence of reward-hacking or the optimization of unintended proxy behaviors.

## 4 Results

In this section, we evaluate the effectiveness of our diagnostic-grounded reward search in discovering rewards that strengthen multi-agent coordination. We begin by introducing the benchmark layouts and the specific coordination challenges inherent in each. We then analyze the objective performance gains across successive generations, highlighting learning dynamics in environments characterized by significant interaction bottlenecks. Finally, we provide a detailed diagnostic analysis to clarify how the discovered shaping signals influence agent interdependence, incentive alignment, and payoff distribution.

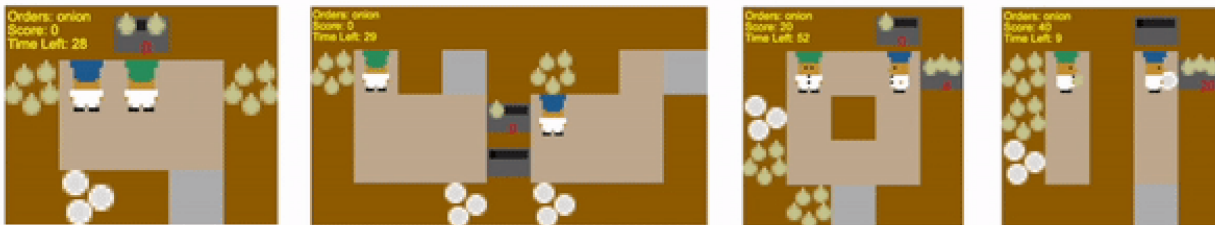


Figure 3: Layouts used in the reported experiments: Cramped Room, Forced Coordination, Coordination Ring, and Asymmetric Advantages.

#### 4.1 Layout Characteristics and Coordination Challenges

Evaluation is performed on the Overcooked-AI cooperative cooking environment [17], where two agents ( $n = 2$ ) must coordinate navigation, resource handling, and timed handoffs to deliver completed soups. The task reward is sparse and is provided only for valid deliveries.

We select four layouts representing a diverse spectrum of dyadic coordination challenges (see Fig. 3): Cramped Room, Forced Coordination, Coordination Ring, and Asymmetric Advantages. Cramped Room is a compact shared workspace in which both agents repeatedly traverse narrow corridors and compete for space. Forced Coordination separates key resources, so progress depends on repeated handoffs and turn-taking at constrained interaction points. Coordination Ring requires synchronized navigation around a ring-like topology with limited passing, which makes deadlocks and mistimed detours costly under sparse feedback. Asymmetric Advantages introduces asymmetric access paths and staging locations, which induces complementary roles while still requiring compatible joint execution.

#### 4.2 Objective Performance and Learning Dynamics

The empirical success of the diagnostic-grounded search is demonstrated by the progression of the sparse task return  $J$  across two successive generations. As reported in Table 1, each search generation is conducted on top of a MAPPO baseline, where candidates are trained from scratch under a fixed computational budget and selected exclusively based on the sparse task objective.

Across all evaluated layouts, we observe a consistent monotonic increase in both sparse returns and successful delivery counts in later generations. The most substantial gains are realized in Coordination Ring and Forced Coordination, where baseline performance is severely constrained by the difficulty of credit assignment under tight interaction bottlenecks. In these scenarios, the baseline agent frequently suffers from coordination failures such as deadlocks, mistimed passing, and handoff synchronization issues.

The synthesized reward programs from later generations effectively bridge this exploration gap by providing dense auxiliary signals for intermediate progress. This acceleration in coordination discovery is clearly reflected in the results: for instance, in the Coordination Ring layout, the Gen 2 candidate achieves a nearly twelve-fold increase in successful deliveries compared to the baseline (7.65 vs. 0.15), while simultaneously reducing invalid deliveries from 11.30 to 0.85. In more straightforward layouts like Cramped Room and Asymmetric Advantages, where the baseline performance is naturally stronger, the framework still yields incremental yet statistically significant improvements within the same compute budget.

Table 1: Final evaluation on four Overcooked layouts.  $J$  denotes sparse return (mean  $\pm$  std across evaluation episodes). Deliveries and invalid deliveries are episode means.

Layout	$J$			Deliveries			Invalid Deliveries		
	Baseline	Gen 1	Gen 2	Baseline	Gen 1	Gen 2	Baseline	Gen 1	Gen 2
Cramped Room	148 $\pm$ 39	180 $\pm$ 25	188 $\pm$ 10	7.40	9.00	9.40	1.15	0.25	0.75
Forced Coordination	32 $\pm$ 14	55 $\pm$ 26	103 $\pm$ 29	1.60	2.75	5.15	0.80	1.25	0.30
Coordination Ring	13 $\pm$ 5	102 $\pm$ 28	153 $\pm$ 24	0.15	5.10	7.65	11.30	3.50	0.85
Asymmetric Advantages	231 $\pm$ 38	322 $\pm$ 36	381 $\pm$ 25	11.55	16.10	19.05	6.15	3.45	1.55

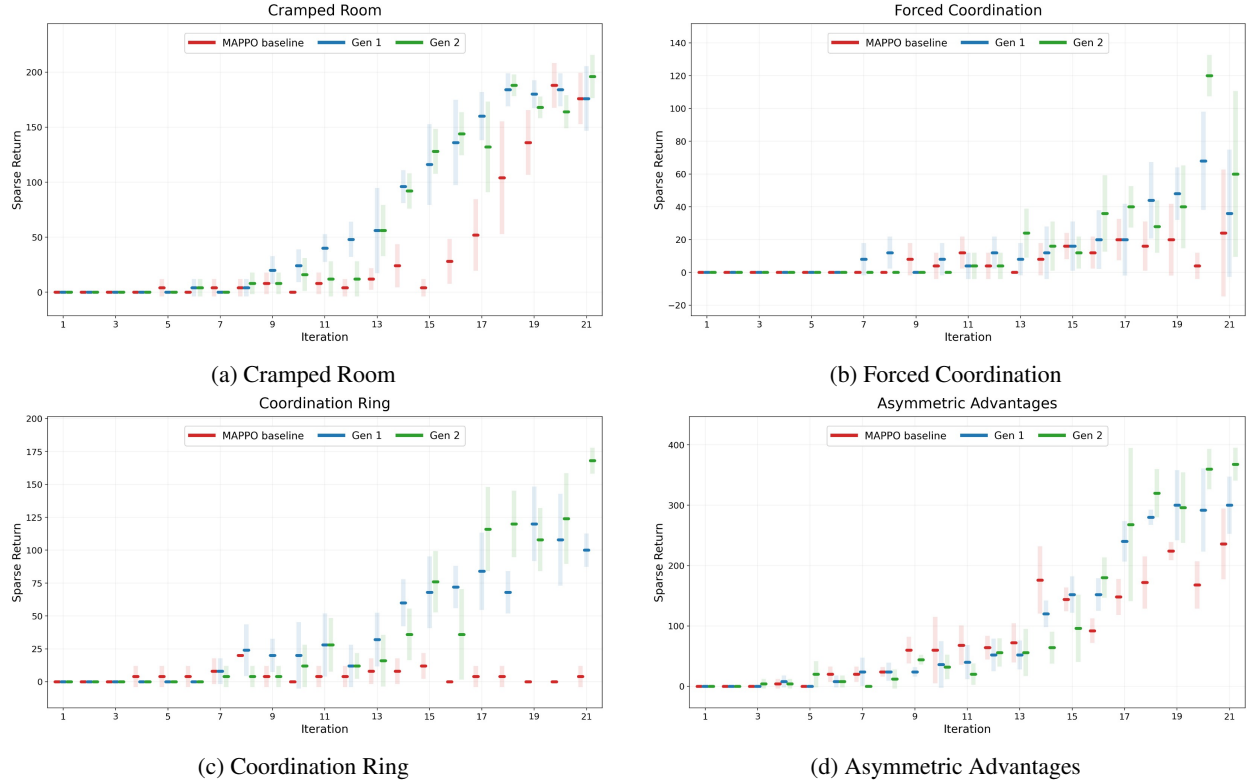


Figure 4: Learning curves of evaluation sparse return  $J$  for the MAPPO baseline and the selected candidates from the first and second generations. Shaded regions indicate variability across evaluation episodes.

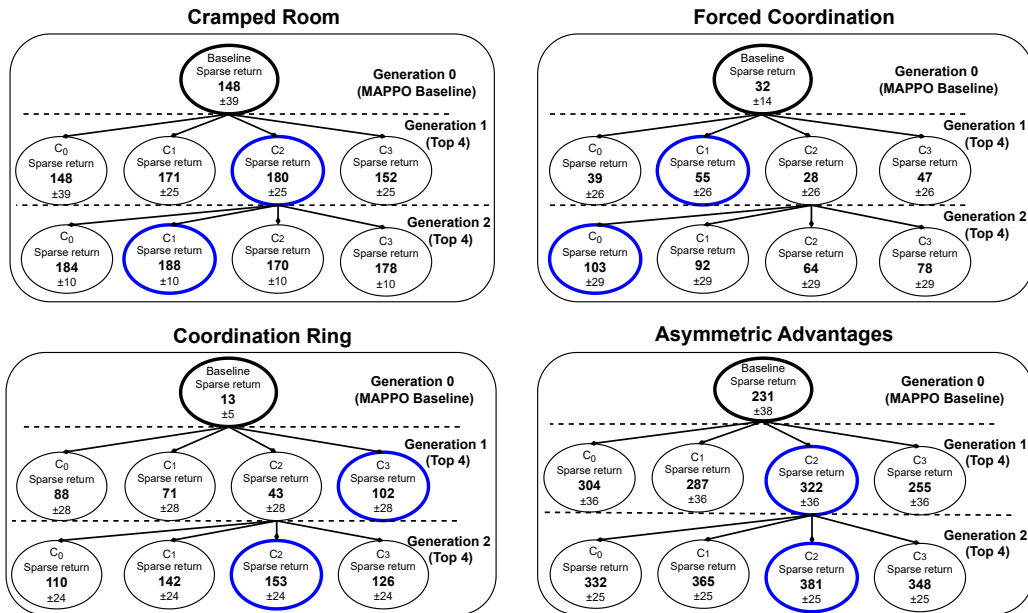
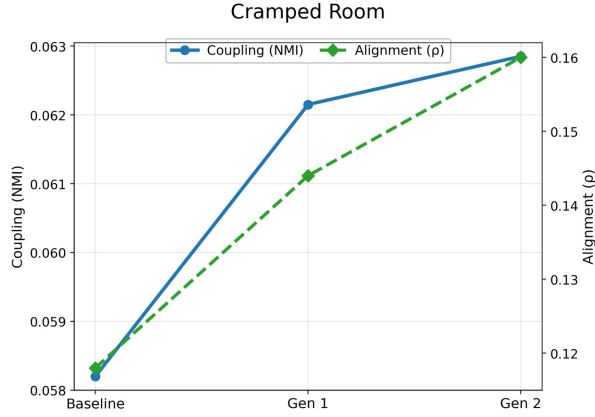
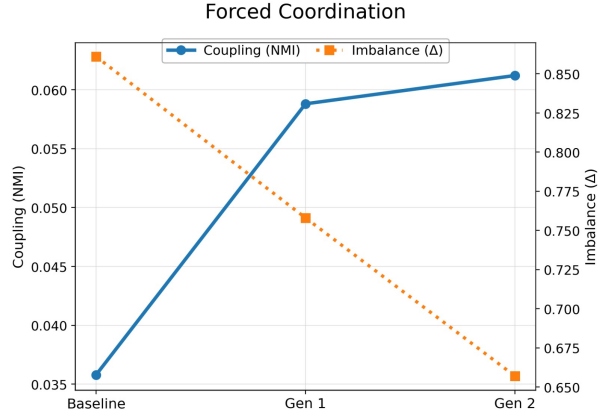


Figure 5: Candidate promotion diagram. Nodes summarize evaluated candidates and objective scores, and edges indicate the promotion path used to condition subsequent generations.

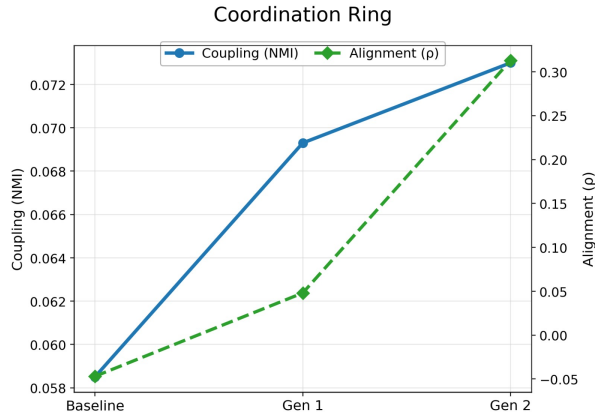
The temporal evolution of agent performance, illustrated through the learning curves in fig. 4, reveals the critical role of synthesized rewards in accelerating coordination. In nearly all layouts, the MAPPO baseline (red) exhibits either



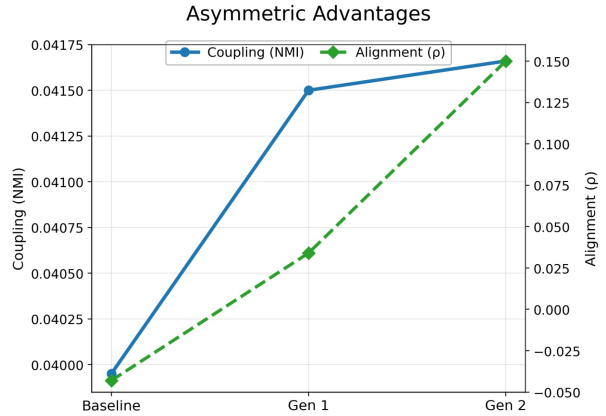
(a) Cramped Room: Increasing trends in Action Coupling (NMI) and Incentive Alignment ( $\rho$ ) signify reduced collision rates in high-density areas.



(b) Forced Coordination: A sharp decline in Payoff Imbalance ( $\Delta$ ) alongside rising NMI indicates a shift from single-agent dominance to equitable workload distribution.



(c) Coordination Ring: Steady growth in  $\rho$  and NMI demonstrates the emergence of synchronized circular motion and temporal waiting behaviors.



(d) Asymmetric Advantages: The upward trajectory in NMI confirms the LLM’s ability to synthesize specialized reward structures for agents with distinct roles.

Figure 6: Empirical Coordination Diagnostics across Overcooked-AI Layouts. The plots illustrate the iterative improvement from Baseline to Generation 2. Blue solid lines represent Action Coupling (NMI), while green dashed lines show Incentive Alignment ( $\rho$ ) and the orange dotted line indicates Payoff Imbalance ( $\Delta$ ).

high variance or premature convergence to suboptimal policies. In contrast, candidates from Generation 1 (blue) and Generation 2 (green) consistently demonstrate higher sample efficiency and asymptotic performance. This trend is most prominent in the Coordination Ring (fig. 4c), where the baseline fails to achieve meaningful progress, while successive search generations progressively unlock higher-order cooperative behaviors, leading to a substantial vertical shift in the reward curves.

To further elucidate the search process, fig. 5 provides a structural lineage of candidate promotion across generations. Each node represents an independent training run of a synthesized reward program, with edges indicating the genealogical path used to condition subsequent LLM prompts. This hierarchical selection mechanism ensures that the search space is effectively pruned toward objective-aligned regions.

The lineage diagrams highlight a robust compounding effect: for instance, in Forced Coordination, the jump from Baseline ( $32 \pm 14$ ) to Gen 2 ( $103 \pm 29$ ) is not merely a result of luck, but the outcome of a structured refinement process where successful shaping strategies from the first generation serve as a foundation for more complex incentives in the second. This iterative improvement confirms that the LLM-proposer can successfully interpret the diagnostic feedback  $d(p)$  from previous iterations to mitigate coordination bottlenecks, such as deadlocks and synchronization failures, which otherwise impede the baseline learner.

### 4.3 Coordination Diagnostics and Shaping Signals

The incentive diagnostics in Sect. 3.3 clarify the evolution of interaction patterns and shaping signals across generations. These quantities represent descriptive summaries from rollouts rather than claims of equilibrium properties. Notably, payoff imbalance and incentive alignment calculations focus on the candidate shaping component  $r_{t,i}^{(p)}$  instead of the shared sparse task reward. Consequently, these metrics capture the distribution of the auxiliary learning signal among agents. Figure 6 reports the mean diagnostic values for candidate pools that satisfy a minimum sparse-return criterion. Two primary trends emerge from these results.

First, the action coupling, measured through NMI, increases across successive search generations in all layouts (Fig. 6a-d). This trend indicates that high-performance reward candidates facilitate more interdependent action selection. In the Overcooked environment, effective performance relies on precise coordinated timing and mutual adaptation. This requirement includes corridor yield maneuvers, the sequencing of interactions at shared stations, and the synchronization of travel paths. The observed increase in NMI remains consistent with the emergence of these strategic dependencies.

Second, incentive alignment ( $\rho$ ) increases in Cramped Room, Coordination Ring, and Asymmetric Advantages (Fig. 6a, c, d). This result indicates that the proposed shaping signals for both agents exhibit a higher positive correlation in later generations. In practice, this pattern aligns with shaping programs that reinforce intermediate progress toward shared subgoals. This alignment prevents the introduction of competing gradients that might destabilize coordination.

A layout-specific pattern is evident in Forced Coordination (Fig. 6b). Because this layout depends on repeated handoffs, shaping that concentrates auxiliary return on a single agent can create asymmetric learning dynamics. In such cases, one agent receives strong gradients, while the other receives weak or noisy guidance. The payoff imbalance diagnostic ( $\Delta$ ) decreases between generations in Forced Coordination, which indicates a more uniform distribution of shaping signals for the selected later-generation candidates. This behavior remains consistent with reward programs that provide guidance for both roles necessary for successful handoffs.

## 5 Conclusion

An objective-grounded approach to autonomous reward program synthesis for cooperative MARL has been presented. In this framework, a large language model generates candidate shaping programs from environment instrumentation. These candidates remain constrained by a formal validity envelope and undergo evaluation under a fixed MAPPO learner. Selection across successive generations depends solely on the sparse task return; consequently, performance improvements are directly related to the intended objective, rather than to the auxiliary shaping signal itself.

Across four Overcooked-AI layouts, later search generations exhibit higher sparse returns and increased delivery counts. The most pronounced gains appear in layouts dominated by interaction bottlenecks under sparse feedback. Diagnostic trends for the shaping component indicate increased action coupling and higher alignment of shaping signals in coordination-heavy tasks. Furthermore, a reduction in the shaping concentration on a single agent is evident in handoff-driven layouts. These results suggest that objective-grounded reward program search can mitigate the burden of manual reward engineering while it yields shaping signals compatible with stable cooperative learning under finite training budgets.

## References

- [1] Michael L. Littman. Markov games as a framework for multi-agent reinforcement learning. In *Proceedings of the Eleventh International Conference on Machine Learning (ICML)*, pages 157–163. Morgan Kaufmann, 1994.
- [2] Andrew Y. Ng, Daishi Harada, and Stuart J. Russell. Policy invariance under reward transformations: Theory and application to reward shaping. In *Proceedings of the Sixteenth International Conference on Machine Learning (ICML)*, pages 278–287. Morgan Kaufmann, 1999.
- [3] Anna Harutyunyan, Sam Devlin, Peter Vrancx, and Ann Nowé. Expressing arbitrary reward functions as potential-based advice. In *Proceedings of the Twenty-Ninth AAAI Conference on Artificial Intelligence (AAAI)*, pages 2652–2658, 2015.
- [4] Sam Devlin, Logan Yliniemi, Daniel Kudenko, and Kagan Tumer. Potential-based difference rewards for multiagent reinforcement learning. In *Proceedings of the 13th International Conference on Autonomous Agents and Multiagent Systems (AAMAS)*, pages 165–172, 2014.
- [5] Sam Devlin, Marek Grześ, and Daniel Kudenko. An empirical study of potential-based reward shaping and advice in complex, multi-agent systems. *Advances in Complex Systems*, 14(2):251–278, 2011.

- [6] Dylan Hadfield-Menell, Smitha Milli, Pieter Abbeel, Stuart Russell, and Anca Dragan. Inverse reward design. In *Advances in Neural Information Processing Systems (NeurIPS)*, 2017.
- [7] Andrew Y. Ng and Stuart J. Russell. Algorithms for inverse reinforcement learning. In *Proceedings of the Seventeenth International Conference on Machine Learning (ICML)*, pages 663–670. Morgan Kaufmann, 2000.
- [8] Brian D. Ziebart, Andrew Maas, J. Andrew Bagnell, and Anind K. Dey. Maximum entropy inverse reinforcement learning. In *Proceedings of the Twenty-Third AAAI Conference on Artificial Intelligence (AAAI)*, pages 1433–1438, 2008.
- [9] Paul F. Christiano, Jan Leike, Tom B. Brown, Miljan Martic, Shane Legg, and Dario Amodei. Deep reinforcement learning from human preferences. In *Advances in Neural Information Processing Systems (NeurIPS)*, 2017.
- [10] Yujing Hu, Wenxuan Wang, Jiahang Tian, Yixiang Wu, Yingfeng Chen, Jianye Hao, Feng Wu, and Changjie Fan. Learning to utilize shaping rewards: A new approach of reward shaping. In *Advances in Neural Information Processing Systems (NeurIPS)*, 2020.
- [11] Ashish Vaswani, Noam Shazeer, Niki Parmar, Jakob Uszkoreit, Llion Jones, Aidan N. Gomez, Łukasz Kaiser, and Illia Polosukhin. Attention is all you need. In *Advances in Neural Information Processing Systems (NeurIPS)*, 2017.
- [12] Tom B. Brown, Benjamin Mann, Nick Ryder, Melanie Subbiah, Jared Kaplan, Prafulla Dhariwal, Arvind Neelakantan, Pranav Shyam, Girish Sastry, Amanda Askell, Ariel Herbert-Voss, Gretchen Krueger, Tom Henighan, Rewon Child, Aditya Ramesh, Daniel Ziegler, Jeffrey Wu, Clemens Winter, Christopher Hesse, Mark Chen, Eric Sigler, Mateusz Litwin, Scott Gray, Benjamin Chess, Jack Clark, Christopher Berner, Sam McCandlish, Alec Radford, Ilya Sutskever, and Dario Amodei. Language models are few-shot learners. In *Advances in Neural Information Processing Systems (NeurIPS)*, 2020.
- [13] Yujia Li, David Choi, Junyoung Chung, et al. Competition-level code generation with AlphaCode. *Science*, 378(6624):1092–1097, 2022.
- [14] Yecheng Jason Ma, William Liang, Guanzhi Wang, De-An Huang, Osbert Bastani, Dinesh Jayaraman, Yuke Zhu, Linxi Fan, and Anima Anandkumar. EUREKA: Human-level reward design via coding large language models. In *International Conference on Learning Representations (ICLR)*, 2024.
- [15] Tianbao Xie, Siheng Zhao, Chen Henry Wu, Yitao Liu, Qian Luo, Victor Zhong, Yanchao Yang, and Tao Yu. Text2reward: Reward shaping with language models for reinforcement learning. In *International Conference on Learning Representations (ICLR)*, 2024.
- [16] Dhawal Gupta, Yash Chandak, Scott M. Jordan, Philip S. Thomas, and Bruno Castro da Silva. Behavior alignment via reward function optimization. In *Advances in Neural Information Processing Systems (NeurIPS)*, 2023.
- [17] Micah Carroll, Rohin Shah, Mark K. Ho, Tom Griffiths, Sanjit A. Seshia, Pieter Abbeel, and Anca D. Dragan. On the utility of learning about humans for human-ai coordination. In *Advances in Neural Information Processing Systems (NeurIPS)*, pages 5175–5186, 2019.